Architecture-Controlled Interaction between Associating Polymers

Arlette R. C. Baljon-Haakman* and Thomas A. Witten

The James Franck Institute, The University of Chicago, 5640 S. Ellis Avenue, Chicago, Illinois 60637

Received October 25, 1991; Revised Manuscript Received January 31, 1992

ABSTRACT: We have developed a Monte Carlo computer simulation to study associating polymer interactions. In our model we treat the associations as geometrical constraints. Each polymer chain contains two "stickers". The chains are treated as lattice self-avoiding random walks. Each sticker is constrained to be adjacent to one other sticker, but the stickers are free to exchange partners. This freedom to exchange results in an attraction between the chains, as anticipated by Cates and Witten (*Macromolecules* **1986,** *19,* 732). We find that in equilibrium the mutual excluded volume of two such chains passes from repulsive to attractive when the ratio of the sticker distance to the chain length is 0.776 ± 0.012 for symmetrically placed stickers and 0.829 ± 0.009 for maximally asymmetrically placed stickers. These results are independent of the chain length (molecular weights 34, 66, and 130): they should apply to real polymers subject to these topological constraints in any good solvent at sufficiently high molecular weight. At these critical placements, the second virial coefficient vanishes and a dilute solution of two sticker chains with doublet sticker interaction is in its Θ state.

1. Introduction

Associating polymers such as ionomers are flexible polymers with a small number of ionic groups randomly attached along the chain.[1] Ionomers typically consist of a hydrocarbon backbone with a few ionic acid groups randomly attached, for example, polystyrene of a molecular weight around 10^5 with about 30 sulfonate groups. The ionic acid groups are neutralized to form salts by cations such as sodium. When dissolved in a nonpolar hydrocarbon solvent, the ionic neutralized acid groups tend to associate or stick together. Scattering data[2] show that the ions cluster into small, long-lived multiplets, but the lifetime of these multiplets is short enough to allow the solution to reach equilibrium readily.[3,4] The multiplets serve to attach chains to themselves and to one another and are responsible for qualitative differences in the macroscopic behavior of an ionomer solution relative to that of an ordinary polymer liquid. For example, under proper conditions a mild shear flow can induce reversible gelation.[5] This effect is thought to be caused by a shift between interchain and intrachain sticking under flow.[6] These ionomer solutions show signs of phase instability, as well.[7] A microscopic aspect of incipient phase instability is seen in scattering studies,[8] which show the tendency for associating polymers to form clusters of chains even in dilute solution. These large clusters give the ionomer solution a phase-separated character.

In this paper we study the equilibrium statistics of these associating polymers in dilute solution. We use a model of Cates and Witten,[9] which appears to contain the essential features needed to understand shear thickening and phase instability. The distinctive molecular feature which appears to give rise to these properties is essentially geometric: it is embodied in the strong tendency of the ionic groups to be together. Thus it is important to understand the effect of this geometric constraint in isolation. This may be done using a simplified model for polymers. Each polymer chain is treated as a lattice self-avoiding random walk with a small number of ionic groups or "stickers" placed along it. Each sticker is constrained to be adjacent to a fixed number, f, of other stickers. The equilibrium state of the solution consists of all configurations of chains which obey these sticker constraints (and those of mutual-avoidance and self-avoidance). Consider two chains with two stickers each and with $f = 2$. Two effects act to cause interaction between the chains. First, in a good solvent the interaction between two self-paired chains (Figure 1a) is repulsive. The range of the repulsion is the size R of each chain (e.g., their radii of gyration). When brought to a separation comparable to their size R, the chains may exchange stickers (Figure 1b). This freedom to exchange results in an increased number of configurations and amounts to an entropic attraction of order kT. Since at such separations the repulsive free energy is also of order kT,[10] the free energies of repulsion or attraction are comparable. Alterations of the sticker placements can alter the balance between repulsion and attraction. Theoretical work[9] shows that near dimension $d = 4$ the net interaction is attractive if all stickers are on the ends of the chains. Since the interaction is repulsive when the stickers are next to each other, there are critical placements for which the repulsive and attractive effects just cancel. In the limit of long chains the critical fractional separation between the stickers is a fixed universal fraction of the chain, independent of the molecular weight and the excluded volume of two monomers.[9]

We expect that a many-sticker chain formed by joining the two-sticker chains end to end is self-repulsive if the repulsion between the constituent two-sticker segments is strong enough. In that case we expect each segment to be predominantly self-paired, so that the sticking is local in the sense shown in Figure 2a. On a scale larger than the typical sticker distance the chain retains its linear topology. We expect that a solution of these chains has the asymptotic scaling properties of an ordinary polymer solution: self-repelling chains asymptotically show self-avoiding random-walk behavior, and they disperse in solution.[11] If instead the sticking is predominantly global (Figure 2b), the chain is self-attractive. Several self-attractive chains in a solution also attract one another. The result should be bad solvation and phase separation.[7]

In this paper we report on computer simulations that check these theoretical predictions. We found as anticipated that the sign of the net interaction, expressed as a second virial coefficient B_2, depends on the placement of the stickers; for a particular critical placement, the interaction vanishes ($B_2 = 0$). We found the critical placement for two situations: symmetric and maximally asymmetric. In the symmetric case both tails have the same length (see Figure 3a). In the asymmetric case one

0024-9297/92/2225-2969$03.00/0

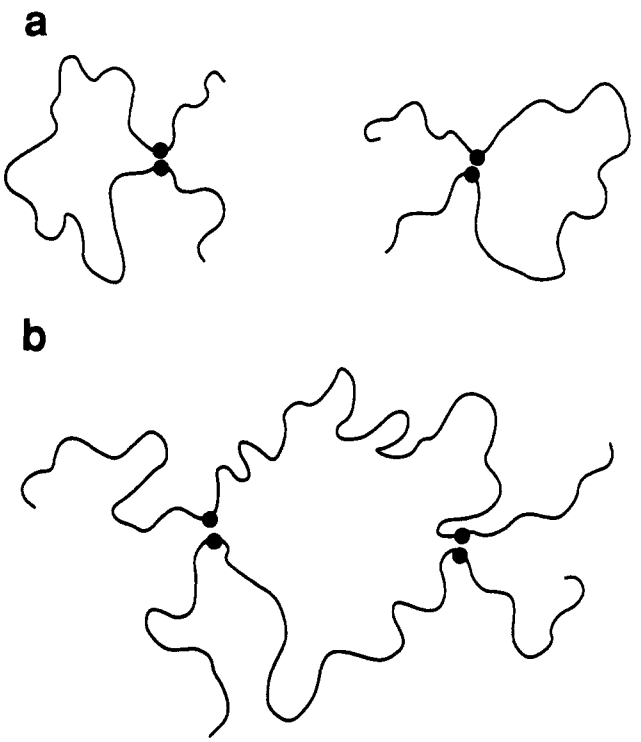

Figure 1. Two self-paired (a) and two cross-paired (b) chains. The stickers are shown as black dots.

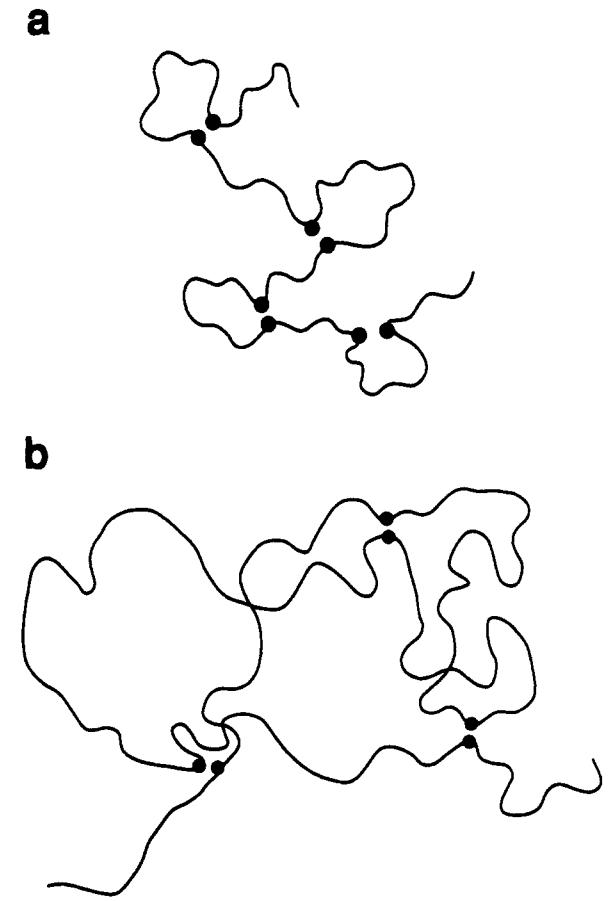

Figure 2. Locally paired state (a) and globally paired state (b). The stickers are shown as black dots.

sticker is fixed at one end point (see Figure 3b). The simulations confirm the prediction that the net interaction depends only on the fractional separation of the stickers along the segments. This dependence is different for the symmetric and asymmetric cases, but for both cases the

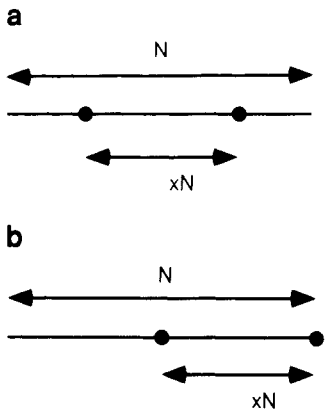

Figure 3. Symmetric (a) and asymmetric (b) sticker placements. The stickers are shown as black dots.

attraction and repulsion balance when the separation between the stickers is roughly 80% of the chain length. Although we determine these interactions using a specific model for the polymer chains, our results must apply to arbitrary polymers of sufficient length in good solvent.

Other studies[12] on associating polymers using geometrical models such as that treated here have also been done. These studies explore general trends of aggregation in many-chain systems. Polymers constrained to have a particular number of self-contacts have been studied analytically by the Cambridge group.[13] Such constraints are similar in spirit to those below, but they do not include the feature of fixing the placements of the enforced contacts along the chain. This feature gives rise to much of the behavior we wish to explore.

2. Simulation Strategy

We want to know how the interaction free energy of a pair of chains depends on the placement of the stickers. The interaction energy can be expressed as a second virial coefficient (B_2). If the interaction between the two chains is repulsive, the second virial coefficient is positive; if the interaction is attractive the coefficient is negative. In general, the second virial coefficient measures how in the dilute region the interaction between many chains affects thermodynamic quantities. For example, the osmotic pressure (Π) is given by

$$\Pi = c + B_2c^2 + O(c^3) \tag{1}$$

Here c is the number of polymers per unit volume. The second term on the right-hand side is a correction to the pressure to take account of interactions. In the dilute region we can neglect $O(c^3)$ terms. As in any solution, we may infer the virial coefficient B_2 from the partition function Z_2 for two chains in a solution of large volume V:[14]

$$Z_2 = Z_1^2(1 - 2V^{-1}B_2 + O(V^{-2})) \tag{2}$$

Here Z_1 is the partition function of an isolated self-paired chain. In our system Z_2 is the sum of self- and cross-linked configuration:[9]

$$Z_2 = Z_1^2(1 - V^{-1}G_0) + Z_{cp} \tag{3}$$

The quantity $Z_1^2V^{-1}G_0$ is the number of self-paired configurations disallowed by the mutual excluded volume of the two chains. Z_{cp} is the total number of allowed cross-paired configurations. The partition function Z_2 is obtained from the simulation of self-paired and cross-paired chains. We may express Z_2 by defining $Z_{cp}(\vec{r})$ as the number of allowed cross-paired configurations in which

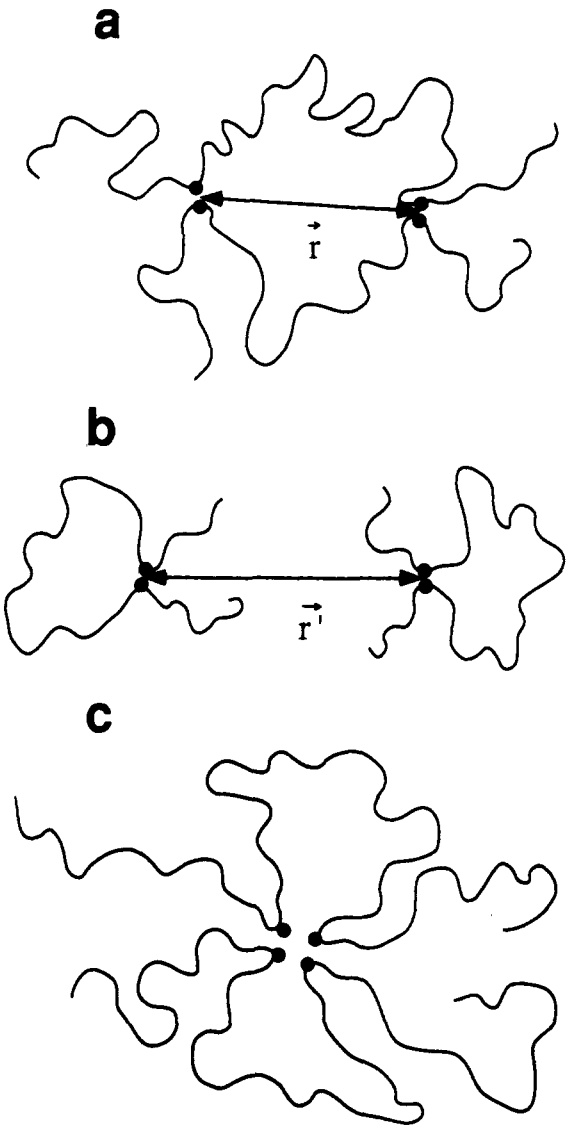

Figure 4. Displacement vectors of the sticker pairs in the cross-paired (a) and self-paired (b) configurations. Each vector connects the middle of the sticker pairs. Part c shows an adjacent pair configuration. This configuration is a self-paired and a cross-paired state.

the displacement vector between the sticker pairs is $\vec{r}$, not counting overall translations (Figure 4a). Similarly, we define $Z_{sp}(\vec{r}')$ as the number of self-paired configurations in which the sticker pairs are at displacement $\vec{r}'$, not counting overall translations of both chains (Figure 4b). Note that the partial partition functions $Z_{cp}(\vec{r})$ and $Z_{sp}(\vec{r}')$ should be equal if the two sticker pairs are adjacent as in Figure 4c. These adjacent pair configurations are used to scale the partial partition functions of the self- and cross-paired configurations, which are in our simulation obtained from two different runs. The self- and cross-paired partial partition functions are scaled so that $\sum' Z_{cp}(\vec{r}) = \sum' Z_{sp}(\vec{r}')$, where the sums are over all adjacent pair configurations.

We want to express B_2 in terms of the partial partition functions. Using $Z_{cp}(\vec{r})$, we may evidently express the full Z_{cp} in eq 3 via

$$Z_{cp} = V\sum_{\vec{r}} Z_{cp}(\vec{r}) \tag{4}$$

The volume factor takes the overall translations into account. In the self-paired configuration the partial partition function $Z_{sp}(\vec{r}')$ goes to a constant at large distances, where the chains do not overlap. This constant

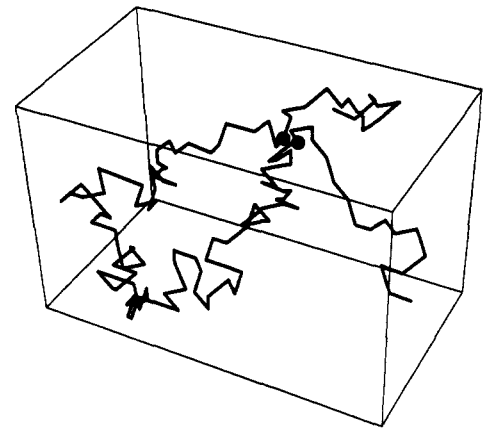

Figure 5. Typical configuration of an isolated self-paired chain in three dimensions. The stickers are shown as black dots.

equals $(Z_1/V)^2$, since Z_1/V is the partition function of an isolated chain not counting overall translations. The total number of disallowed states in which the sticker pairs are at displacement $\vec{r}'$ is

$$V[(Z_1/V)^2 - Z_{sp}(\vec{r}')] \tag{5}$$

and the total number of disallowed states $Z_1^2V^{-1}G_0$ is found by summing on $\vec{r}'$:

$$Z_1^2V^{-1}G_0 = V\sum_{\vec{r}'}((Z_1/V)^2 - Z_{sp}(\vec{r}')) \tag{6}$$

We note that the summand vanishes for r' much larger than the polymers, so that the sum is independent of the volume of the system. From eqs 3, 4, and 6

$$Z_2 = Z_1^2 - V\sum_{\vec{r}'}((Z_1/V)^2 - Z_{sp}(\vec{r}')) - V\sum_{\vec{r}} Z_{cp}(\vec{r}) =$$

$$Z_1^2\left[1 - V^{-1}\sum_{\vec{r}'}\left(1 - \frac{Z_{sp}(\vec{r}')}{(Z_1/V)^2}\right) - V^{-1}\sum_{\vec{r}}\frac{Z_{cp}(\vec{r})}{(Z_1/V)^2}\right] \tag{7}$$

B_2 is obtained from eqs 2 and 7

$$B_2 = 1/2\left[\sum_{\vec{r}'}\left(1 - \frac{Z_{sp}(\vec{r}')}{(Z_1/V)^2}\right) - \sum_{\vec{r}}\frac{Z_{cp}(\vec{r})}{(Z_1/V)^2}\right] \tag{8}$$

The quantities $Z_{cp}(\vec{r})$, $Z_{sp}(\vec{r}')$, and Z_1/V are measured in our simulation. The $Z_{sp}(\vec{r}')$ data go to a constant at large $\vec{r}'$. This constant equals $(Z_1/V)^2$ and takes care of the overall normalization.

3. Simulation Details

A configuration consists of two random-walk chains on a simple cubic lattice with the following properties: (a) Each step of a random walk goes arbitrarily to a neighbor, second neighbor, or third neighbor site. (b) No two steps of the walks occupy the same lattice site. (c) Two particular monomers at specific points along the chain are designated as stickers. (d) Each sticker is adjacent to one other sticker. (e) In addition, we only consider configurations in which one sticker is at the origin. This eliminates configurations that differ by a mere overall translation. A typical configuration of an isolated self-paired chain is shown in Figure 5.

In our Monte Carlo algorithm we use a bead-jump mechanism described in ref 13 to relax each segment separately. A segment is either a chain between the two sticker pairs or a chain tail. These bead jumps sample the chains with fixed sticker positions. To change the relative displacements between the sticker pairs, we include a second type

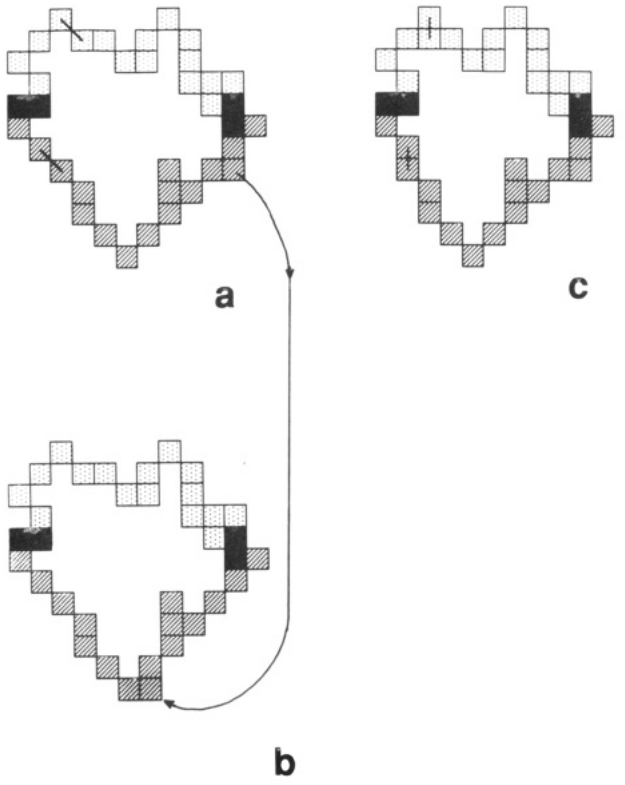

Figure 6. Two-dimensional configuration of a cross-paired state before (a) and after a successful bead jump (b) and macromove (c). The stickers are black; the two chains are dotted and striped. In the bead jump one monomer is removed and inserted at a new point on the same chain. In the macromove the two marked parallel bonds of a are replaced by those in c.

of move. These "macromoves" are rigid translations of a part of the chains. We discuss these moves in detail below.

Each bead jump consists of two steps. First we choose an arbitrary monomer and try to remove it. The removal is allowed if the new bond between its neighbors is smaller than the maximal bond length ($\sqrt{3}$). Second, if the removal is successful, we pick an arbitrary bond and try to place the removed monomer between the monomers that are connected by this bond: we choose a site at a distance smaller than the maximal bond length from one of the monomers connected by the bond and try to place the removed monomer on that site and to replace the old bond by two new bonds, so as to insert the monomer in the chain. The try is successful if the picked site is not occupied and if the new bond lengths do not exceed the maximum bond length. If the try is not successful, we place the monomer back in its original place. This procedure is slightly modified if the monomer is inserted at an end of a chain, since then there is only one new bond. The bead-jump move is shown in Figure 6.

This bead-jump mechanism has been proven[15] to be a statistically unbiased sampling procedure and to reproduce well-known scaling results on single chains and loops. The computation time τ for a single chain of molecular weight N to relax is empirically[15] of the order N^3. This τ is defined, e.g., as the time for the chain to diffuse its own radius of gyration (R_g). An estimate of the optimal ratio of macromoves over bead jumps in our simulation is obtained by requiring that the time for an isolated sticker pair to diffuse a distance R_g is of order τ. The sticker pair would diffuse a distance R_g in a computation time $\tau_1(R_g/l)^2$, if we would try to move an isolated sticker pair a distance l every τ_1 bead jumps. This gives

$$\tau \approx N^3 \approx \tau_1(R_g/l)^2 \tag{9}$$

This implies that τ_1 should scale with N as

$$\tau_1 \approx N^3/R_g^2 \approx N^{3-2\nu} \tag{10}$$

where ν is the Flory exponent. We try to do a macromove every $N^{3-2\nu}$ bead-jump steps. Since the exponent is positive, the macromove attempts are rare. We checked our estimate by measuring the decay of the autocorrelation of the radius of gyration for a chain with stickers attached at the ends. Our findings confirm a relaxation time on the order of N^3 bead jumps. If the stickers are in other positions, the relaxation time is shorter. In most runs the molecular weight of the polymers is 66 and the relaxation time is at most $66^3 \approx 2^{18}$ bead jumps. To obtain sufficient equilibrium data, we run at least 2^{28} bead-jump steps, or longer than approximately 1000 relaxation times. The runs for the molecular weight 130 polymers are 2^{30} bead-jump steps or 500 relaxation times.

The macromove for the self-paired chains is commonly used in Monte Carlo simulations of many-chain systems:[12,16] the move is a simple rigid translation of one of the chains through a finite distance and is accepted if no overlapping among the chains occurs. If we move the chain through an arbitrary distance, all allowed transitions for given internal configurations occur with equal likelihood and the thermodynamic ensemble is uniformly sampled. We use instead an importance sampling method.[17] Each sticker pair displacement $\vec{r}'$ has a certain weight $w(\vec{r}')$. In every move we attempt a new displacement to $\vec{r}'$, with probability $w(\vec{r}')$, and we move the chain so that the new sticker pair displacement is $\vec{r}'$. Thus displacements with higher weights are sampled proportionately more often. In order to obtain the partial partition functions $Z_{sp}(\vec{r}')$, we have to correct the number of times we find the sticker pairs at displacement $\vec{r}'$ in our simulation $\tilde{Z}_{sp}(\vec{r}')$ for the weight:[17]

$$Z_{sp}(\vec{r}') = w^{-1}(\vec{r}')\,\tilde{Z}_{sp}(\vec{r}') \tag{11}$$

The weight function is chosen as follows: In order to obtain enough sampling in the adjacent pair configurations, approximately 30% of the moves are attempts to place the sticker pairs in an adjacent pair configuration. In 5% of the moves we place the mobile polymer in a position where there is no overlap possible. We need this information in order to obtain Z_1/V. At other distances the weight function is obtained from the Gaussian function

$$w(\vec{r}') = e^{-s|\vec{r}'|^2} \tag{12}$$

The spring constant s is adjusted so that we sample most of the time in the region of interest (r' smaller than the polymer size).

To make a macromove for the cross-paired chains, one selects at random a pair of bonds. If these bonds are not parallel, the move fails. We attemp the move so many times that on the average every $N^{3-2\nu}$ bead jumps a parallel bond is selected. If the bonds are parallel, we try to replace them by new parallel bonds in a different direction. This translates one part of the structure and one sticker pair as shown in Figure 6. Since the adjacent pair configurations occur only rarely, we use again an importance sampling method. The weight function is given by

$$w(\vec{r}) = \begin{cases} e^{-s|\vec{r}|^2} & \text{if } |\vec{r}| \le r_m \\ e^{-sr_m^2} & \text{otherwise} \end{cases} \tag{13}$$

Here r_m is the position of the peak of the partition function $Z_{cp}(|\vec{r}|)$. The spring constant s is adjusted so that there is equal sampling at distances smaller than r_m.

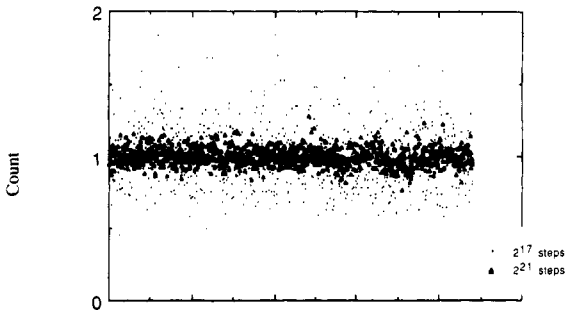

Figure 7. Detailed balance for two chains of molecular weight 3, forming a loop. The y-axis gives the relative number of times each configuration is found. Each point on the x-axis represents a different allowed configuration. The fluctuations in the number of times each configuration is found are statistical, and they decrease if the run time increases.

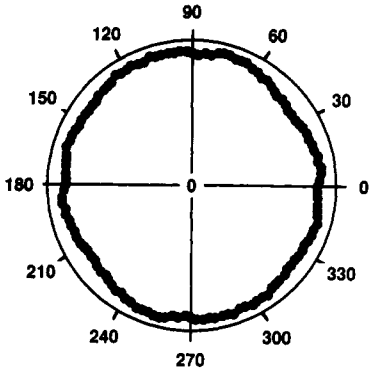

Figure 8. Time-averaged distance between opposite monomers. The sticker pairs are at 0 and 180°. The average distance between two opposite monomers is 10.73 lattice spaces. That between the two sticker pairs is 10.59 lattice spaces.

We checked these macromoves for cross-paired chains by treating the special case of loop polymers: all stickers are at the ends, so that the two polymers form a loop. First we checked for detailed balance: each allowed configuration should be visited an equal amount of time.[17] In Figure 7 we plot the number of times each configuration is found versus the allowed configurations for polymers of molecular weight 3. Shown are data for 2^{17} and 2^{21} bead-jump runs. The data show that the fluctuation is less (factor 2.5) in the longer run, as expected. In the second test we obtain the (time) average distance between two opposite monomers (molecular weight 66). In Figure 8 we plot these distances in a radial graph. The sticker pairs are at 0 and 180°. The (time) average distance between opposite monomer pairs is approximately the same for the sticker pairs as for the others, as it should be. Its average over all different monomer pairs is 10.73 lattice spaces. The (time) average distance between the sticker pairs is 10.59 lattice spaces. The slight discrepancy might be due to the fact that the stickers are restricted to be nearest neighbors unlike the other bonds. Finally, we checked that the radius of gyration scales with molecular weight as expected. In Figure 9 we plot the radius of gyration versus molecular weight on a double log scale. The slope of a linear fitted line is 0.60 ± 0.03, in agreement with the Flory exponent: $\nu \approx 0.6$.

To obtain data in two dimensions, we use an effective two-dimensional lattice: there are only two layers in the third direction. The second layer allows the chains to access all possible configurations for a certain sticker pairing. It would, for example, not be possible to obtain both configurations of Figure 10 in one run, if there is only one layer. This is due to the fact that the sticker pairs can only move by rigid translation: their spatial direction is fixed.

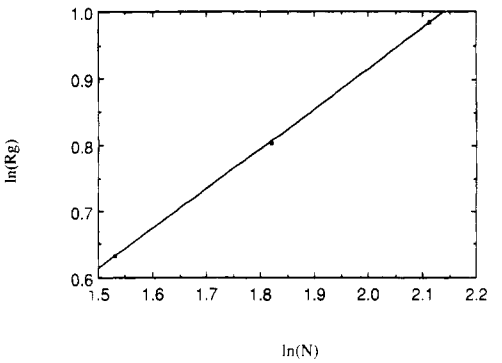

Figure 9. Scaling of the radius of gyration with distance, for two polymers forming a loop. The slope, obtained from a linear least-squares fit is 0.60 ± 0.03, in agreement with the Flory exponent (0.6).

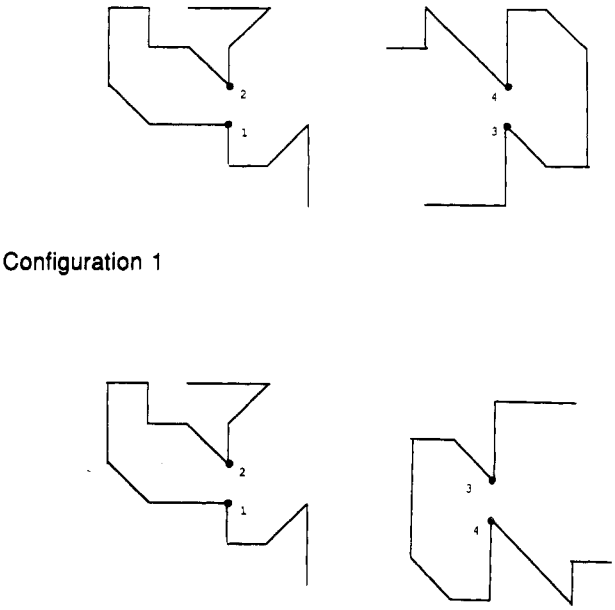

Figure 10. Two typical self-paired configurations in two dimensions. The stickers are numbered. Since the sticker pairs can only move by rigid translation, the direction of the bond between stickers 1 and 2 and that between 3 and 4 are fixed. This means that in our algorithm it is not possible to sample both configurations in one run. The same problem arises in the cross-paired state.

4. Results

Figure 11 shows the normalized second virial coefficient $\hat{B}_2$ for two polymer chains in three dimensions with symmetrically placed stickers. For reasons explained later we plot $\hat{B}_2$ versus $y \equiv x^{2.16}$, where x is the ratio of the sticker distance to the chain length. The data for the different chain sizes (molecular weights 34, 66, and 130) are normalized so that $\hat{B}_2(y) = 1$ at $y = 0$. We checked that the unnormalized excluded-volume data scale with chain length as $B_2 \approx N^{3\nu} \approx N^{1.8}$. At $y = 0$ we found that $B_2 \approx N^{(1.80\pm0.05)}$. The error bars shown in Figure 11 are obtained as follows: The error in a $\hat{B}_2$ data is obtained from the errors in both of its parts: the self- and cross-paired contributions. The error in each part is the statistical error in each run: the value of the sum in a full run minus that in a half-run divided by the square root of 2. In parts a and b of Figure 12 we plotted the $\hat{B}_2$ data versus chain length for $y = 0.23$ and $y = 0.54$. In both

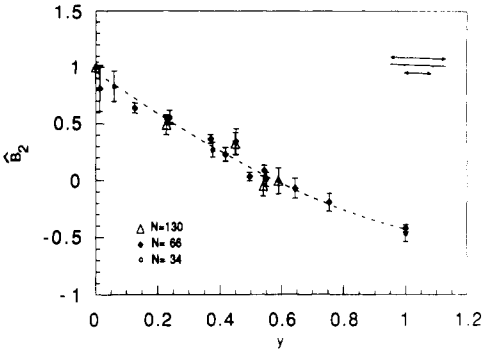

Figure 11. Normalized second virial coefficient $\hat{B}_2$ versus sticker placement for symmetrically placed stickers. $y \equiv x^{2.16}$, where x is the distance between the stickers divided by the length of one chain. The values for the different chain lengths (34, 66, and 130) are scaled so that they are unity at $x = 0$. A third-order polynomial fit is shown: $\hat{B}_2 = (0.96 \pm 0.3) - (1.92 \pm 0.11)y + (0.3 \pm 0.2)y^2 + (0.2 \pm 0.6)y^3$.

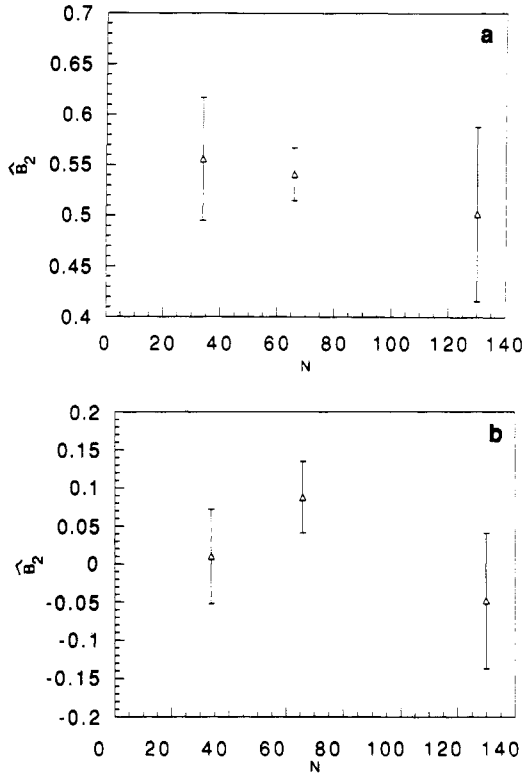

Figure 12. Normalized second virial coefficients versus chain length for symmetrically placed stickers separated a distance 0.631 (a) and 0.754 (b) of the chain length. Within three statistical fluctuations the data for different chain sizes are equal.

cases the data are within error bars independent of the chain length. The superposition of the data for different chain sizes confirms the expected asymptotic scaling. Moreover, the $\hat{B}_2$ versus y data in Figure 11 show that as y increases the chains cross from self-repelling to self-attractive behavior as anticipated. From the data we want to find the critical sticker placements y_c for which there is no net mutual interaction between the chains ($\hat{B}_2 = 0$). In order to calculate y_c, we want to fit a polynomial through the data. According to ref 9 at low x, $\hat{B}_2(x) - \hat{B}_2(0) \approx x^{\nu(d+\theta_2)}$. Here θ_2 is an exponent describing certain interior correlations within a self-avoiding chain; its value has been measured to be approximately 0.67[18] so that $\nu(d + \theta_2) \approx 2.16$. Evidently the $\hat{B}_2$ versus y data in Figure 11 are consistent with the prediction, since $\hat{B}_2$ shows linear behavior for small y. A third-order polynomial fit gives a minimum value for χ^2 per degree of freedom (1.1). From the coefficients we find $y_c = 0.58 \pm 0.02$ or $x_c = 0.776 \pm 0.012$.

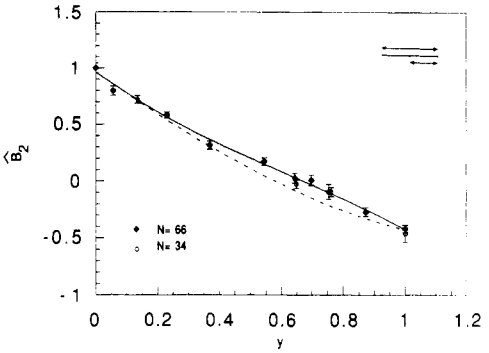

Figure 13. Normalized second virial coefficient versus sticker placement for maximally asymmetrically placed stickers. $y \equiv x^{2.16}$, where x is the distance between the stickers over the chain length. The values for the different chain lengths (34 and 66) are scaled so that they are unity at $x = 0$. The solid line is a third-order polynomial fit: $\hat{B}_2 = (0.97 \pm 0.2) - (2.01 \pm 0.07)y + (1.3 \pm 0.3)y^2 - (0.7 \pm 0.4)y^3$. The dashed line shows the fit to the symmetric data points in Figure 11.

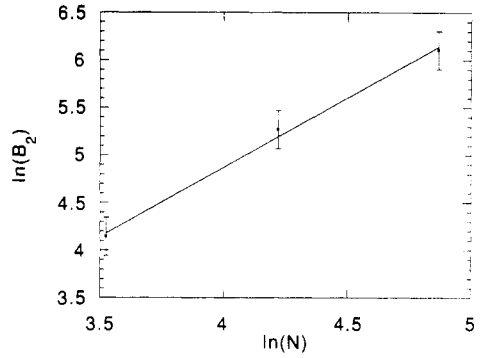

Figure 14. Second virial coefficient (B_2) versus molecular weight (N) in two dimensions. A linear least-squares fit shows that B_2 scales with N as $B_2 \approx N^{1.46 \pm .04}$ in agreement with the expected Flory scaling (1.5).

If we place the stickers maximally asymmetrically, we obtain the data shown in Figure 13. Note that in this case two different cross-paired states are possible. Again the partial partition functions were linked together at the adjacent pair configurations. We plot $\hat{B}_2$ versus $y \equiv x^{\nu(d+\theta_1)}$. The values of θ_2 and θ_1 found experimentally are approximately equal,[18,19] so that again $y = x^{2.16}$. A third-order polynomial fit gives $y_c = 0.668 \pm 0.015$ or $x_c = 0.829 \pm 0.009$ (χ^2 per degree of freedom is 0.9).

In two dimensions we found that for all sticker placements the net mutual interaction between the chains is repulsive. Even when the stickers were placed at the chain ends, the attraction due to cross-pairing was not enough to compensate for the intrinsic mutual repulsion of the chains: $\hat{B}_2(x=1) \approx 0.37$. We verified these results using chains of molecular weights 34, 68, and 130. We checked that in the loop configuration the second virial coefficient scales with molecular weight as a volume: $B_2 \approx N^{2\nu} \approx N^{1.5}$. In Figure 14 we plot the B_2 data versus molecular weight on a double log scale. The slope of a linear fit is 1.46 ± 0.04.

5. Discussion

We found that y_c shifts from 0.58 to 0.668 if we place the stickers maximally asymmetrically instead of symmetrically. These values are obtained from two separate third-order fits through the symmetric and asymmetric data. Since at $y = 0$ and $y = 1$ the symmetric and asymmetric configurations are identical, it would have been

better to fit polynomials through both data sets, constraining the fits to go to the same points at $y = 0$ and $y = 1$. Figure 13 shows the fitted polynomials through the asymmetric and symmetric data sets. Within error bars the values of the critical placements are the same as those found from two separate fits. We note that in Figure 13 at low y the fitted polynomials are almost identical. The linear coefficients of the polynomials are the same within error bars. The quadratic terms are different, and this results in the small difference in the values of the critical points: In the maximally asymmetric configuration the critical distance between the sticker pairs is slightly higher than that in the symmetric configuration. We claim that the asymmetric and symmetric critical distances x_s and x_a should obey the following inequality:

$$\frac{1}{2}(1 - x_s) \leq (1 - x_a) \tag{14}$$

Let us call the molecular weights of the tail ends $T_s(N)$ and $T_a(N)$ for the symmetric and asymmetric configurations at their critical point. Clearly (see Figure 3)

$$T_s(N) = \frac{1}{2}(1 - x_s)N \tag{15}$$

and

$$T_a(N) = (1 - x_a)N \tag{16}$$

Suppose we start with the asymmetric chain at its critical point and form a second tail on each chain using monomers from the centerloop segments, to produce symmetric chains. These chains evidently have a net repulsion, since the centerloops have been shortened in favor of the tails. Thus, to regain the critical state, the tails must be shortened: $T_s(N) \leq T_a(N)$. Using eqs 15 and 16, we obtain the inequality in eq 14. The critical values we found are indeed in agreement with this inequality. For arbitrary, not symmetrically or totally asymmetrically sticker placements, we expect x_c to be between its symmetric and totally asymmetric values. In general, we expect a critical line of sticker placements versus symmetricality. Figure 13 suggests that increased asymmetry leads to increased repulsion $\hat{B}_2$, since for most y the asymmetric line lies above the symmetric line. However, we have not been able to prove this. Finally, if we would allow the stickers to dissociate, $\hat{B}_2$ should increase with the decreasing strength of the sticker attraction.

We expect that our results hold for real chains in real solvent if the sticking energy is high enough, so that the associating groups are only a small fraction of the time dissociated. Furthermore, the function $\hat{B}_2(x)$, being a property of asymptotically long polymers, is insensitive to molecular detail or polymer type.[20] In particular, the ratio of physical quantities should be universal near the fixed point ($N = \infty$).[20] In order to test this universality, we altered the random walks so that only steps of length $\leq \sqrt{2}$ were allowed. This reduces the root-mean-square bond length by 20%. For both bond lengths we simulated chains of molecular weight 66 with stickers at the ends and we determined the ratio of disallowed self-paired states $Z_1^2 V^{-1} G_0$ over allowed cross-paired states Z_{cp}. If we allow bond lengths up to the $\sqrt{3}$, we find for this ratio 0.67 ± 0.02; if the maximum bond length is $\sqrt{2}$, we find 0.63 ± 0.02. These data are identical within the statistical uncertainty. The fact that we find a universal value for a relatively short chain (molecular weight 66) is in agreement with the fact that the renormalized $\hat{B}_2$ values seem to be converged for the chain sizes we used (34–130 monomers) within the statistical errors.

It would be interesting to test our findings experimentally. One thing to measure would be $\hat{B}_2$ as function of the sticker placement from, e.g., osmotic pressure versus concentration measurements in the dilute regime for two-sticker chains. We expect our predictions for $\hat{B}_2$ to apply quantitatively to polymers that satisfy the topological constraints assumed here. Each polymer must have two sticker groups at specified positions on the chain. Each sticker must form a labile bond with one other. A possible realization is anionically polymerized polystyrene with carboxylic acid residues attached to the phenyl side groups at two points. In hydrocarbon solution each acid group is expected to associate strongly with another one via hydrogen bonding.[21] The bonding must be strong enough so that dissociated groups are rare.[22] Since the equilibrium constant of dimerization[23] is approximately 10^4 cm^3/g, the sticker concentration must be at least 10^{-4} g/cm^3. At a fixed polymer concentration c ($c \leq c^*$) the probability to find dissociating groups can be reduced by an overall decrease of the polymer molecular weight. On the other hand, the bonding must also be specific, so that association of more than two acid groups is rare. Unfortunately, carboxylic acid groups can be expected to show some nonspecific attraction of one pair for another, since paired groups themselves are polarizable moieties in a nonpolar medium. Chemical intuition suggests that this association is rare at sticker concentrations of approximately 10^{-4} g/cm^3. Stronger primary association could be obtained by replacing each acid group with two such groups attached to the same or adjacent monomers. These must be oriented so that they cannot hydrogen bond with each other. The two groups then act effectively as a single sticker which is stronger than a single acid group.

Since at the critical distances the second virial coefficient of the chains vanishes, the polymer solution is in its Θ state: the associations between the chains make it possible to obtain the Θ state in a robust way, which is relatively insensitive to the temperature of the solution or solvent composition.

6. Conclusion

We found that in equilibrium the mutual interaction between two two-sticker chains passes from repulsive to attractive when the distance between the stickers increases. This might give rise to a new interesting way to attain the Θ state for a dilute polymer solution. The required balance is achieved using geometrical constraints which depend only on the chain architecture. Until now we studied the simplest case: two chains with two stickers each and doublet sticker interaction. To explore the potential of this mechanism, it should be studied for more realistic and general situations: chains with many stickers and stickers which associate in triplets, quadruplets, etc. In the first instance we plan to study how the mutual interaction of our two-sticker chains is related to the self-interaction of many-sticker chains. We expect that higher order interactions of the two-sticker segments will renormalize the second virial coefficient of the segment interaction.[24]

Acknowledgment. We thank Michael Murat for his help with the program code. This research was conducted using the Cornell National Supercomputer Facility, a resource of the Center for Theory and Simulations in Science and Engineering (Cornell Theory Center), which receives major funding from the National Science Foundation and IBM Corp., with additional support from New York State and members of the Corporate Research

Institute. This work was supported by the Material Research Laboratory at The University of Chicago under NSF Grant DMR 88-19860.

References and Notes

(1) MacKnight, W. J.; Earnest, T. R., Jr. *J. Polym. Sci. Macromol. Rev.* **1981**, *16*, 41.
(2) Williams, C. E.; Russell, T. P.; Jerome, R.; Horrion, J. *Macromolecules* **1986**, *19*, 2877.
(3) Agarwal, P. K.; Garner, R. T.; Lundberg, R. D. *Macromolecules* **1984**, *17*, 2794.
(4) Broze, G.; Jerome, R.; Teyssie, P.; Marko, C. *Macromolecules* **1983**, *16*, 996.
(5) Duvdevani, I.; Lundberg, R. D. U.S. Patent, Statutory Invent. Regist.; U.S. 363 H1 DATE: 871103 APPLICATION: U.S. 808117 (851212).
(6) Witten, T. A.; Cohen, M. H. *Macromolecules* **1985**, *18*, 1915.
(7) Agarwal, P.; Garner, R. T.; Graessley, W. W. *J. Polym. Sci., Polym. Phys. Ed.* **1987**, *25*, 2095.
(8) Pedley, A. M.; Higgins, J. S.; Peiffer, D. G.; Rennie, A. R.; Staples, E. *Polym. Commun.* **1989**, *30*, 161.
(9) Cates, M. E.; Witten, T. A. *Macromolecules* **1986**, *19*, 732.
(10) Pincus, P. A.; Witten, T. A. *Macromolecules* **1986**, *19*, 2509.
(11) des Cloizeaux, J.; Noda, I. *Macromolecules* **1982**, *15*, 1505.
(12) Balazs, A. C.; Gempe, M.; Brady, J. E. *J. Chem. Phys.* **1990**, *92*, 2036.
(13) Ball, R. C.; Cates, M. E. *J. Phys. A* **1984**, *17*, L531.
(14) Reichl, L. E. *A Modern Course in Statistical Physics*; University of Texas Press: Austin, TX, 1980.
(15) Murat, M.; Witten, T. A. *Macromolecules* **1990**, *23*, 520.
(16) Curro, J. G. *J. Chem. Phys.* **1974**, *61*, 1203.
(17) Binder, K.; Heermann, D. W. *Monte Carlo Simulations in Statistical Physics: An Introduction*; Springer-Verlag: Berlin, 1988.
(18) des Cloizeaux, J.; Jannink, G. *Polymers in Solution: Their Modelling & Structure*; Oxford University Press: Oxford, U.K., 1990.
(19) Guttmann, A. J.; Sykes, M. F. *J. Phys. C: Solid State Phys.* **1973**, *6*, 945.
(20) Freed, K. F. *Renormalization Group Theory of Macromolecules*; Wiley: New York, 1987.
(21) Schuster, P.; Zundel, G.; Sandorfy, C. *The Hydrogen Bond: Recent Developments in Theory and Experiments*; North-Holland Publishing Co.: Amsterdam, The Netherlands, 1976.
(22) Though carboxylic acid groups may stick strongly in this sense, they do not appear to stick strong enough to produce dramatic rheological effects.[3]
(23) Bulmer, J. T.; Shurvell, H. F. *J. Phys. Chem.* **1973**, *77*, 256.
(24) Khoklov, A. R. *J. Phys. (Paris)* **1977**, *38*, 845.